Sheet Pile Interlocks and Ring Beam Installation Effects on the Performance of Urban Cofferdams

A. Felipe Uribe-Henao, S.M.ASCE[1]; and Luis G. Arboleda-Monsalve, Ph.D., M.ASCE[2]

[1]Research Assistant, Dept. of Civil Engineering and Construction Engineering Management, California State Univ., Long Beach, CA 90840. E-mail: Andres.Uribehenao@student.csulb.edu
[2]Assistant Professor, Dept. of Civil Engineering and Construction Engineering Management, California State Univ., Long Beach, CA, 90840. E-mail: Luis.Arboleda@csulb.edu

Abstract

Urban cofferdams are made of steel sheet piles that are structural sections with interlocking systems used to build a continuous wall. These systems are constructed by driving sheet piles, assembling subsequent sheet pile sections, and installing ring beam bracings as the excavation proceeds. The interlock connections between sheet pile sections tend to have a natural slack which leads to additional deflections of the support system. It is only after some deformation that the natural slack of the interlocks and sheet pile-to-steel ring beam connections close their gaps and the bracing system is fully engaged. These features on urban cofferdam behavior are presented parametrically in three-dimensional numerical analyses. Large differences on the computed lateral wall deformations are presented when ignoring these installation effects. Disregarding these pre-excavation construction effects conceal the fundamental reason for the resulting ground deformations in the construction of urban cofferdams and deep excavations.

INTRODUCTION

Urban cofferdams built with sheet piles are typically used as temporary structures to retain the earth and in offshore applications to exclude water from the work place. These structures have been used mainly in offshore applications but its use expanded to construction of high-rise structures in major populated areas. Its construction process involves driving sheet piles followed by the installation of bracing systems as the soil is excavated. Numerous sources of movement impact the adequate performance of these type of structures. In this paper, the compliance of the connections between different sheet pile segments, called sheet pile interlocks, is studied and their contribution to the lateral deformations of the urban cofferdam is assessed. These connections producing slippage between sheet piles have been studied by several researchers. Clough and Kuppusamy (1985) developed a plane strain fully-coupled soil-structure interaction model to study the performance of a cellular cofferdam. As opposed to the case presented here, sheet pile interlocks for cellular cofferdams are subjected to tension instead of compression. The authors modeled the interlocks using multi-linear springs to improve the computed response in light of observed performance, and proposed the E-ratio concept to capture the out-of-plane flexibility caused by the interlocks. This concept introduces in the model an arbitrary reduction of the out-of-plane modulus of elasticity of the sheet pile. An E-ratio of 0.03 matched the observed performance of the Lock and Dam 26 cellular cofferdam. Crawford and Byfield (2002) evaluated the bending of U-shaped sheet piles, also known as Larssen sheet piles, and discussed that the slippage of one pile relative to another causes a reduction of 70% of the elastic bending stiffness.

DESCRIPTION OF OMPW URBAN COFFERDAM

The test bed for this study is the excavation made for the 53-story reinforced concrete building, the One Museum Park West (OMPW) in Chicago (IL). The basement levels of this structure were constructed using a combination of excavation support systems. The excavation for the installation of reinforced concrete central core walls was developed using a circular cofferdam made of sheet piles and segmental curved steel ring beams. The excavation for the rest of the building, which is out of the scope of this paper, was made using a top-down method. The depth of cut for the cofferdam was approximately 15 m. Cycles of soil removal and lateral bracing were completed following conventional bottom-up excavation techniques using a 24.25 m diameter cofferdam made of PZC-18 steel sheet pile sections. The sheet piles were driven to an approximate elevation of -16 m CCD (Chicago City Datum) and four steel ring beams were installed as the construction progressed. These steel ring beams served as the internal lateral bracing system for the cofferdam and were made of segmental curved W14 sections connected using bolted steel plates. Steel brackets welded to the sheet piles were used to support the steel ring beams and provided radial bracing that increased the stiffness of the support system. The steel ring beams are supported approximately every 6.35 m in the circumferential direction. The W14x176 topmost steel ring beam is located at 2.74 m from the top of the cofferdam, which is larger than the recommended location of the first support in typical bottom-up construction (Puller 2003). The remaining steel ring beams made of W14x193, W14x211, and W14x257 steel sections are located at elev. -1.83, -4.57, and -7.92 m CCD, respectively. The height and diameter of the cofferdam were 19.8 and 24.25 m, respectively. The bottom of the cut is reached at -10.5 m CCD and the wall is embedded in the soil up to -16.15 m CCD. The construction of the cofferdam was reported by Finno et al. (2014) to have contributed about 30% of the total settlements resulting from this project. More attention should be paid to design these intermediate stages of support for deformation control of these type of cofferdams.

The ground surface around the cofferdam was leveled to elev. 3.7 m CCD to guide the installation of the sheet piles. After interlocking and driving the sheet pile segments, the soil was excavated inside of the cofferdam. The first level of steel ring beam supports was installed at elevation 0.91 m CCD, which is approximately 3.0 m below the ground surface. Next, three additional supports were installed at approximate intervals of 3 m as the excavation advanced to brace the system until the bottom of the cut was reached at elev. -10.5 m CCD. At the bottom of the cut, a 2.5 m thick reinforced concrete mat foundation was placed and was structurally connected to 2.75 m diameter reinforced concrete caissons bearing on rock. The mat foundation served as the support of 0.75 m thick reinforced concrete shear walls that formed the central core of the structure. The sheet pile walls and steel ring beams remained in place as the core walls were constructed. The subsurface conditions in the OMPW site consist of a compacted granular fill from elev. 3.6 to 0.9 m CCD which is on top of a 2.5 m thick medium to stiff clay crust. Soft-to-medium clay layers from elev. -1.83 to -14.6 m CCD commonly referred as Blodgett and Deerfield underlie this layer. Stiff to hard clays were founded from elev. -14.6 to -19.3 m CCD. Further details about the subsurface conditions are provided by Finno et al. (2014).

NUMERICAL MODELING OF OMPW URBAN COFFERDAM

The cofferdam geometry of the OMPW building is presented in Figure 1. The figure illustrates the main structural system composed of sheet piles and ring beam bracings made of four different steel hot-rolled wide-flanged sections. Figure 1b shows the structural model of the cofferdam using the finite element program SAP2000. The main objective of this model is to study the resulting deformations from the abovementioned compliances during the construction of the cofferdam, mainly the sheet pile interlocks and sheet pile-to-steel ring beam connections.

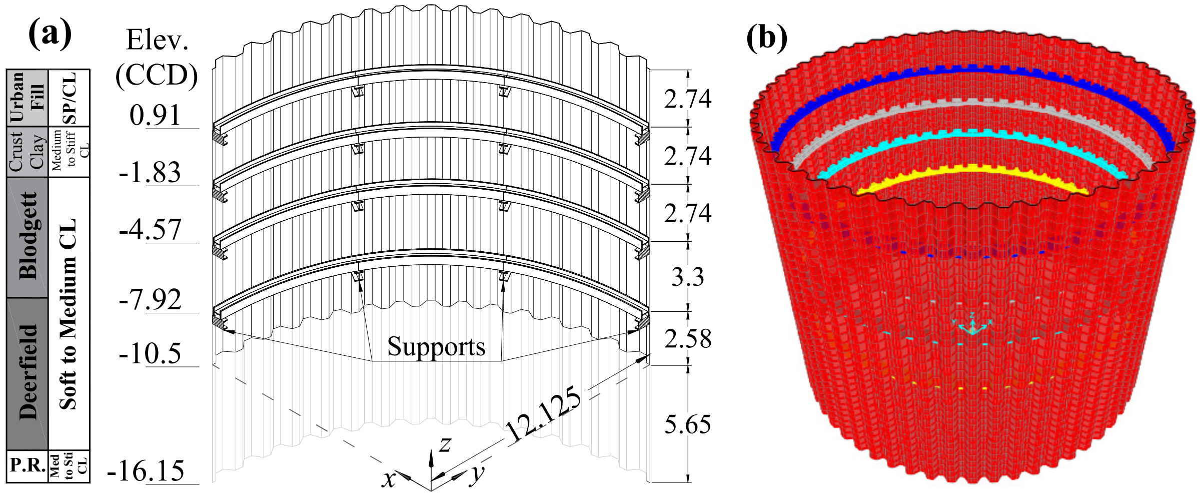

Figure 1. Elevation view of the OMPW cofferdam: a) schematic view of the cofferdam (units given in meters) and b) 3D numerical model of the cofferdam using SAP2000.

The modeling components of the sheet pile, steel ring beams, sheet pile interlocks, and connection sheet pile-to-steel ring beams are presented in Figure 2a. The sheet pile segments are composed of PZC-18 modular pieces, which are interlocked during the driving process with ball-socketed interlocks located every 0.635 m. About 120 segments were interlocked in the cofferdam. The modeled cross section is presented in Figure 2b. The thickness of the sheet pile section was increased from the actual value of 9.5 to 12 mm to account for the contributions of the interlock portions to the overall area and moment of inertia. The moment of inertia and area per unit length of wall in the model were 7.37 cm^4/m and 156.2 cm^2/m, respectively. Differences with respect to the actual values provided by the manufacturer were only 3% smaller. The structural steel material of the sheet piles and steel ring beams was assumed homogeneous and linear elastic with Young's and shear moduli of 200 and 77 GPa, respectively.

The sheet pile segments were modeled using thin shell elements with a four node formulation that uses the combined theory of membrane and plate bending behavior. The membrane behavior uses an isoparametric formulation while the plate bending behavior uses an out-of-plane rotational stiffness and a translational stiffness perpendicular to the plane of the shell. Every element has its own local coordinate system numbered as 1, 2, and 3 following the right-hand rule. The steel ring beams are modeled as linear-elastic frame segments spaced every 0.635 m and are restrained to displacements in the vertical direction but free to rotate and displace in any other direction. The connections between segments are assumed to be continuous and rigid, fully transmitting forces and displacements across the steel ring beams. The self-weight of the supports and steel ring beams was neglected.

Figure 2c presents the link objects used to model the sheet pile interlocks. Recall that the cofferdam is formed with several PZC segments interlocked with ball-socketed type connections. Those connections are modeled with rotational and translational springs in the bending and axial planes. The stiffnesses, denoted as k_R and k_T, were modeled with multilinear link objects. Figure 2d shows the modeling strategy to include the gap at times left open during construction between the sheet pile wall and steel ring beam. Equal displacement properties were assigned to joints at the same level of node j to prevent sheet pile nodes overpassing steel ring beam nodes because of the large flexibility of the sheet pile wall in relation to the ring beams. Those joints are connected by means of a link object with a linear elastic stiffness k_w that potentially accounts for the stiffness of any filler material used to close those gaps. At first, when the gap is open, the force acting in the link is zero. Once the gap closes, the force acting in the gap is calculated using the Hook's law based on the relative displacement between joints j and i. The maximum gap magnitude, e, was estimated to be about 50 mm.

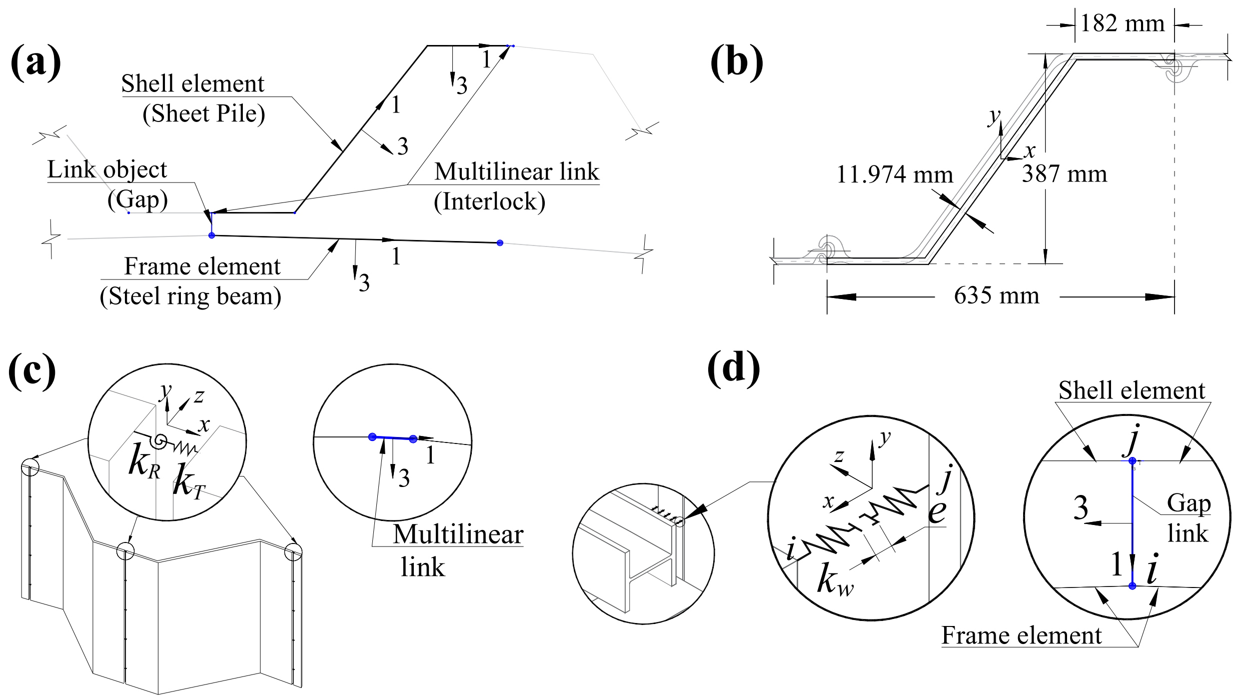

Figure 2. Definition of the objects used in the numerical model: a) modeling components, b) PZC-18 cross section and equivalent section, c) sheet pile interlock modeling, and d) sheet pile-to-steel ring beam connection (gap).

The cofferdam in the SAP2000 numerical model was loaded perpendicularly to the sheet piles with computed active earth and water pressures developed as the excavation proceeded. A separate model to determine these loads was developed in PLAXIS 3D with the hypoplasticity model parameters calibrated by Arboleda-Monsalve (2014). The stage construction in the SAP2000 numerical model started by installing the sheet piles, loading the cofferdam with at-rest earth and water pressures, and activating the internal nonlinear soil resistance. The excavation was simulated by removing the corresponding nonlinear soil resistance, updating the active earth and water pressure loading as computed with a separate model developed in PLAXIS 3D, and activating the ring beam bracings. As the ring beams are installed, the retaining wall increases its stiffness causing a redistribution of the internal forces and stresses particularly at the unexcavated passive resistance zone of the cofferdam. The soil resistance to inward wall movements caused by the excavation is modeled with nonlinear springs assigned to each soil layer of the cofferdam: medium dense sandy fill, soft-to-medium compressible clays, and stiff clays. However, since SAP2000 performs load-controlled analyses, a reduction of the forces acting on the springs only is achieved when their stiffness is updated as the excavation proceeds. Thus, the nonlinear load-deformation response for these soils in SAP2000 was determined using an iterative approach based on the results obtained from the geotechnical program PLAXIS 3D. The approach implemented to match the passive resistance of both programs starts by calculating the loads in the cofferdam computed from PLAXIS 3D and simultaneously the soil reaction forces in the soil springs from SAP2000. The differences between both programs are reduced once the nonlinear soil response is corrected in SAP2000 taking the results of PLAXIS 3D as the reference values. This process is repeated until the passive resistance to inward wall movement at the bottom of the excavation is the same in both programs. The final load-deformation curves for each excavation phase used in the analyses are presented in Figure 3 and are specific to each excavation phase. In the figure, it is observed how the passive resistance of the soil is reduced as the excavation proceeds.

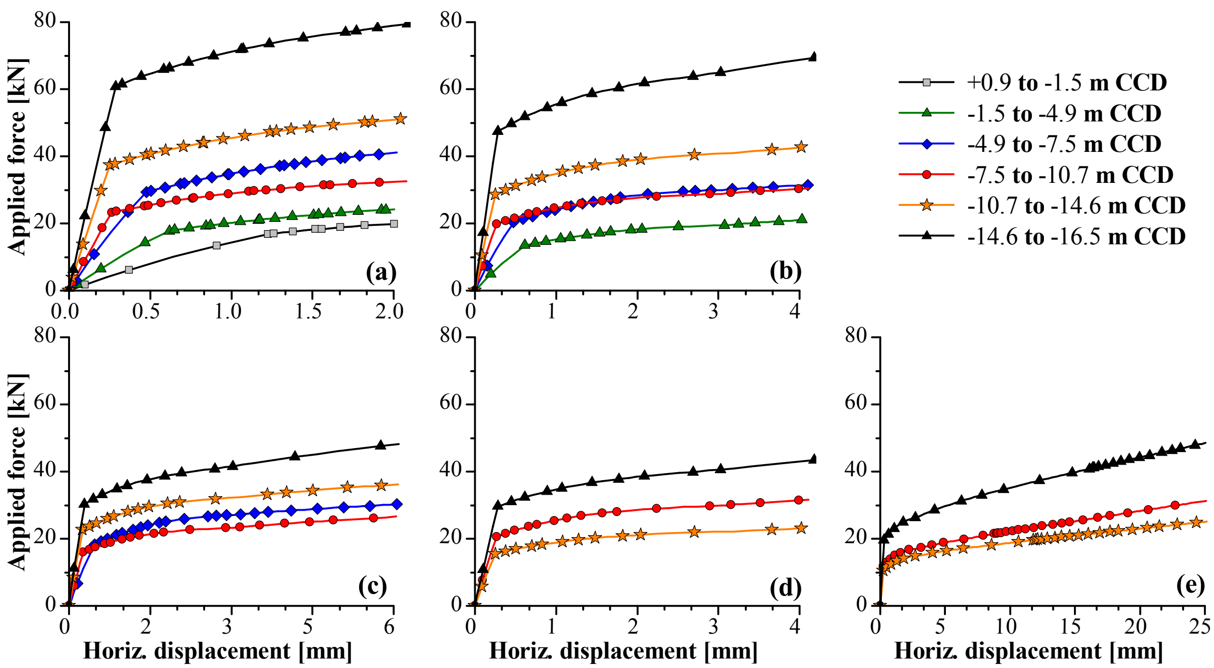

Figure 3. Nonlinear soil resistance to inward wall movements for the different depths and excavations to ring beam: a) 1; b) 2; c) 3; d) 4; and e) bottom of cut.

Sheet pile interlocks develop frictional forces arising from contact of different steel components and steel-to-soil interaction. A separate model shown in Figure 4 was developed in PLAXIS 2D to study the soil-sheet pile interlock interaction when these connections are subjected to compression. This model consisted on reproducing the *in situ* stress field (i.e., vertical effective stresses and confining pressures) with a K_0 initial stage. Then, compressive loads were applied to close an opening of 9 mm and fully engage the structural steel material of the sheet piles. This opening was selected to match the spacing of PZC-18 ball-socketed interlock connections. The Mohr-Coulomb constitutive soil model was used for the urban fill and glacial clays confined in the interlock connections. The large stresses and strains of the soil developed inside the sheet pile interlock indicated that a model like Mohr-Coulomb should be sufficient to describe this soil failure mechanism and provide a reasonable estimate of the soil stiffness.

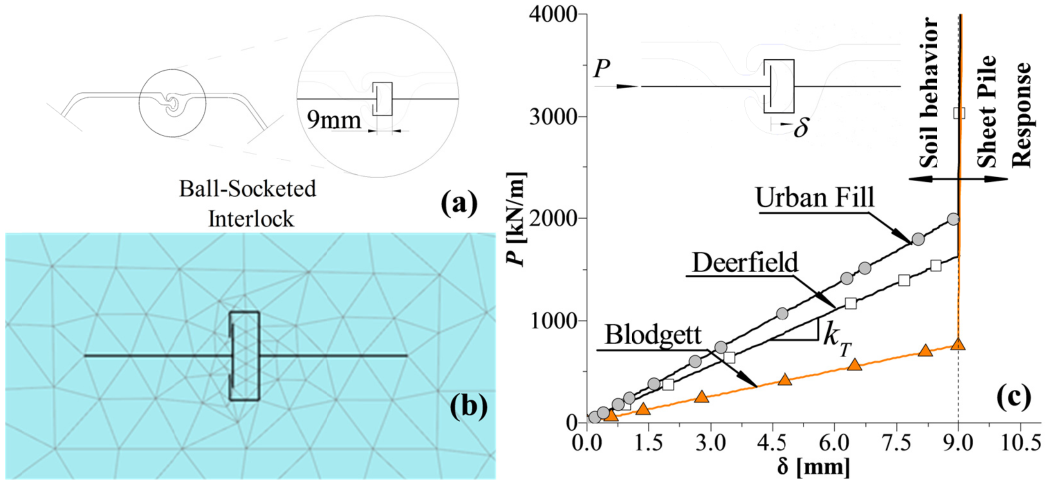

Figure 4. Numerical model of the soil-sheet pile interlock interaction: a) slack in the interlocked connections, b) numerical model in PLAXIS 2D, and c) force-deformation curves computed for each soil layer.

Table 1 presents the soil properties used to study the soil-sheet pile interlock interaction. The modulus of elasticity for Blodgett and Deerfield clays was computed using the Janbu hypoelastic model (Janbu 1963) with modulus number and exponent taken as 890 and 1.26, respectively (Lade and Kim, 1988). The parameters for the urban fill were taken from Calvello (2002). The force-deformation curves are presented in Figure 4c. The connection deforms and responds with an initial stiffness typical of these type of soils under *in situ* confining pressures until the interlock closes. Then, as shown with a sharp increase in the slope of force-deformation curves, the structural steel material of the interlock components is engaged.

RESULTS OF THE NUMERICAL ANALYSES

Parametric studies are carried out to evaluate the proposed effects. Figure 5 presents the computed lateral deformations of the sheet pile wall as the excavation proceeds. A lower bound is presented using a perfect interlock connection (i.e., infinite rotational and translational stiffness $k_R = k_T = \infty$) and perfect contact of the steel ring beams with the sheet pile wall during construction (i.e., $e = 0$). An upper bound is presented with the interlock translational stiffnesses taken from Figure 4c and assuming negligible rotational stiffness and sheet pile-to-steel ring beams separated 50 mm, as observed in some connections in the OMPW cofferdam. The stiffness of the sheet pile wall is increased at the locations of the steel ring beams as shown with the slope variations in the deformed shape. It is only until the 50 mm gap is closed that the lateral bracing provided by the ring beams is fully engaged. Leaving gaps in the installation of the ring beams mobilizes large amounts of soil strength and stiffness. The maximum computed lateral wall deflections of the upper bound case are four times of those computed for the lower bound. Those differences are mostly attributed to the sheet pile-to-steel ring beam gaps. Figure 5 also shows the lateral deflections measured in the field with an inclinometer installed about 5m away from the cofferdam. It is observed in the figure that since the lateral wall deformations are affected by the construction and installation of the ring beams and the translational and rotational stiffness of the interlock connections as presented in this paper, the observed lateral wall deformations lie within the lower and upper bounds, being the lower bound case a more reasonable approximation of the actual cofferdam behavior.

Table 1. Mohr-Coulomb parameters used for soil-sheet pile interlock interaction model.

Symbol	Parameter name	Soil Type		
		Urban Fill	Blodgett	Deerfield and Park Ridge
E (kPa)	Modulus of elasticity	17,620	40.54	76.85
ν	Poisson ratios	0.33	0.2	0.2
G (kPa)	Shear modulus	6,624	16.89	32.02
E_{oed} (kPa)	Oedometer modulus	26,110	45.04	85.39
c'_{ref} (kPa)	Cohesion	19.1	0	0
ϕ' (°)	Drained friction angle	35	25.3	31.7
γ_{sat} (kN/m^3)	Saturated unit weight	18.9	18.9	18.9
ψ (°)	Dilatation angle	5	0	0

The internal forces acting on the sheet pile interlock vary depending upon the location, type of connection, and relative position of the interlock components inside of the ball-socketed connection. This space left in the interlock tends to delay the activation of the structural steel of the sheet pile wall to respond to the excavation-induced loading. For instance, if the interlock connection under compressive loading is open, the soil stiffness needs to be mobilized first before the structural steel is activated. Thus, under compression the connection responds as shown in Figure 4 and under tension responds directly with the stiffness of the structural steel. This is labeled as Case I in Figure 6. If the interlock space after installation is closed for compressive loads, the response of the connection is as depicted in Case II. An intermediate case is labeled as Case III, in which the interlock components are halfway and bilinear soil curves for tension and compression are proposed. The influence on the computed lateral wall deflections of the relative position of the interlock components for infinite rotational stiffnesses of the interlock connections is shown in Figure 6a. The computed lateral wall deformations are shown from the inner nodes of the PZC section (i.e., nodes closer to the steel ring beams). The relative position of the interlock components is shown to have little influence in the resulting lateral wall deformations.

The largest wall deformations are expected to occur for Case I because these cofferdams are mainly subjected to compressive stresses. However, the results showed that the largest deformations occurred for Case II in which the connections are closed and the structural steel material of the sheet pile is immediately engaged under compressive loading. This occurs because the inner connection of the sheet pile (i.e., interlock connection closer to the steel ring beams) is subjected to tensile stresses arising from flexure as the excavation progresses instead of compressive stresses. This behavior can only be captured if the actual PZC cross section is modeled. Using an equivalent rectangular cross section, as typically assumed in the numerical analyses of deep excavations with sheet piles, ignores the fact that interlocks are subjected to either tensile or compressive stresses, depending upon their position with respect to the neutral axis of the sheet pile. The slight variations of the lateral deformations resulting from the position of the interlock components (Figure 6a) proves that other factors such as the soil and structural model parameters and the loading conditions applied to the numerical model have a more significant effect in the lateral deformations.

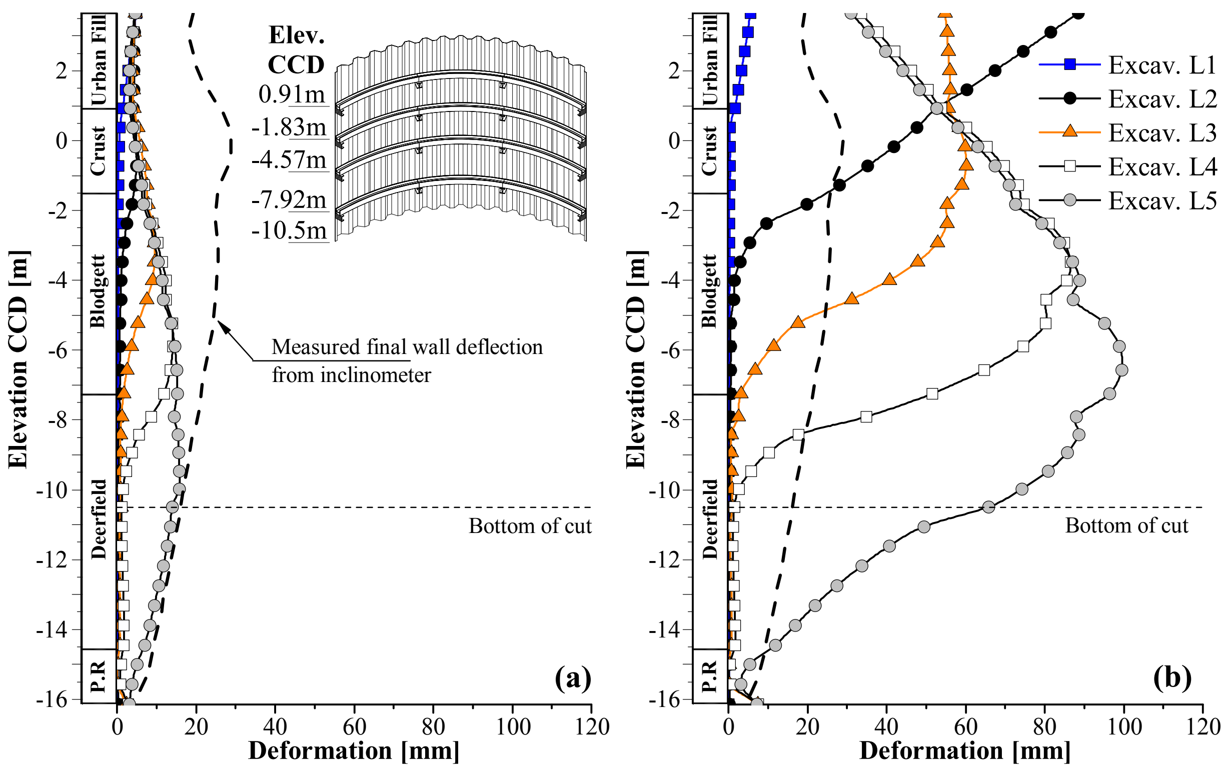

Figure 5. Computed variation of lateral sheet pile wall deflections: a) lower bound and b) upper bound

The influence of the interlock rotational stiffness on the computed lateral wall deflections is shown Figure 6 The interlock rotational stiffness is shown in relation to the flexural stiffness of the sheet pile wall per unit length computed as EI/L= 69.8 kN m/rad/m. Perfectly pinned and perfectly fixed cases and intermediate values of 20 and 80% of the flexural stiffness are shown in the figure (i.e., k_R = 0, 0.2EI/L, 0.8EI/L, and ∞). For those calculations, the gap between sheet pile and steel ring beams is assumed closed and the interlock relative position Case III is used. The results show that sheet pile walls with low values of the interlock rotational stiffness are more flexible. Small differences of about 5% or less are computed in the lateral wall deformations at the connections between the sheet pile wall and steel ring beams. This is because at those points, deformations are mostly controlled by the stiffness of the ring beams. However, differences of about 23% are computed in the lateral wall deformations for the portions between steel ring beams.

Figure 6c shows the effect of leaving gaps between sheet piles and steel ring beams during construction. The results are computed using the interlock relative position Case III, interlock rotational stiffnesses $k_R = 0$ and ∞, and different sheet pile-to-ring beam gap values (e) varying from 0 to 50 mm. As expected, the lateral wall deformations increase as the gap values increase and the rotational stiffnesses of the interlocks reduce. Gaps left open between sheet piles and steel ring beams strongly affect the overall cofferdam behavior, as shown by the magnitude of the lateral wall deflections at the elevations of RB-3 and RB-4. These large deep-seated movements occur at the elevations of the compressible soft-to-medium clay layers at the project site. The resulting wall deformations at the bottom of cut and the location of the fixity point of the sheet pile wall are not significantly affected by this effect. Not only the design stiffness of the lateral bracing system is key in the successful performance of urban cofferdams, but also the installation of lateral bracings needs to be carefully completed in the field minimizing gaps that reduce the capabilities of the bracings to prevent excavation-induced deformations. As opposed to more rigid excavation support walls, sheet piles are very flexible and the control of movements highly depend on the lateral bracing system.

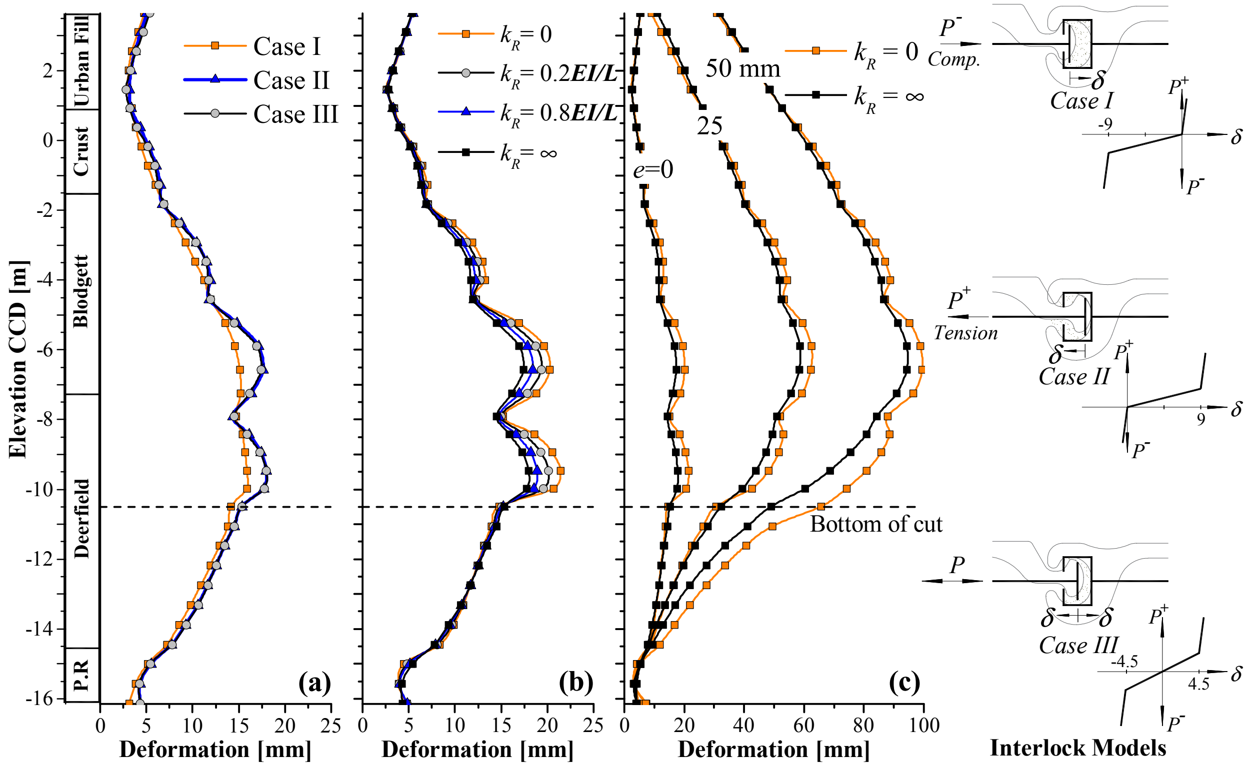

Figure 6. Computed variation of lateral wall deflections at the end of construction for different: a) relative positions of the interlock components, b) interlock rotational stiffness, and c) gaps between sheet piles and steel ring beams.

CONCLUSIONS

The interlocked connections between sheet pile sections tend to have a natural slack, which leads to additional deflections of the support system. Interlocks are subjected to either tensile or compressive stresses which cannot be accurately calculated using equivalent rectangular cross sections. Variations of about 23% in the computed lateral wall deflections were obtained by assuming either negligible or infinite rotational stiffnesses of sheet pile interlocks. Slight differences of about 8% in the computed deformations were found for different relative positions of the ball-socketed ends of the interlocks. It was also shown parametrically that very large lateral wall deformations result from leaving gaps between sheet piles and steel ring beams. The steel ring beam bracings are engaged only after those gaps are closed, which reduces the capability of the steel ring beams to brace the support wall. The lateral wall deformations computed when including these gaps left open during construction represent four times the deformation obtained when ignoring these installation effects. Adding wood blocks or any other type of filler material to close those gaps, preloading the ring beams, or using reinforced concrete ring beams cast in direct contact with the sheet pile walls are alternatives to prevent additional deformations arising from these construction effects. The performance of cofferdams is significantly affected by the effects studied in this paper.